**acta physica slovaca vol. 51 No. 2, 151 – 162** **April 2001**

# NEW GENERATION OF DEVICES FOR ALL-OPTICAL COMMUNICATIONS

**I. Glesk**
*Department of Optics, Faculty of Mathematics and Physics, Comenius University, Mlynská dolina, F-2, 842 48 Bratislava, Slovakia*

**R. J. Runser, P. R. Prucnal**
*Department of Electrical Engineering, Princeton University, Princeton, NJ 08544, USA*

Received 18 September 2000, in final form 3 January 2001, accepted 4 January 2001

To increase the transmission capacity of future communication networks is becoming very critical. This task can only be accomplished by taking advantage of optical networks where multiplexing techniques such as Dense Wavelength Division Multiplexing (DWDM) and Optical Time Division Multiplexing (OTDM) are employed. To avoid electronic bottlenecks a whole new generation of ultrafast devices is needed. To fulfill these needs a new class of all optical devices has been proposed and developed. By taking advantage of the nonlinear dynamics in semiconductor optical amplifiers in combination with the fiber interferometers a new generation of ultrafast all-optical demultiplexers and wavelength converters has been demonstrated. Other switching technologies are also promising for the future. The latest technologies in the area of micro-machining have created very attractive low cost MEMS. Recently announced use of bubble technology for all-optical switching might also lead to the development of next generation large scale switching fabrics. This paper is an overview of the recent development in these areas.

PACS: 42.79.Sz, 42.79.Ta

## 1 Introduction

The explosive growth of the Internet has placed new demands on the bandwidth of the physical transport layer of the backbone network. While optical technology has begun satisfying the demand with high bandwidth dense wavelength division multiplexed (DWDM) point-to-point links, switching and routing packets has been performed using electronic hardware. Although electronics is sufficient for packet routing today, the tremendous growth in data traffic predicted over the next 5 years will push electronics to its fundamental limits. Current electronics that switch and route packets on the Internet rely upon integrated silicon (Si), gallium arsenide (GaAs), and indium phosphide (InP) devices. From a physics perspective, it is not likely that these technology will achieve terahertz speed needed for switching in the future Internet. New techniques are needed to alleviate the potential electronic bottleneck. It appears that optical technology will

be the only technology capable of achieving multi-terabit/second communications. For future generations of optical networks to utilize the full bandwidth of optical fiber, we expect data rates on each individual channel in DWDM networks to exceed the practical bit-rate of the driving electronics. To accommodate such high data rates, individual wavelength channels may be composed of modulated, picosecond mode-locked laser pulses from each data source. These new systems will optically aggregate traffic from many users into unique, closely spaced time slots to achieve extremely high data rates on each wavelength. By utilizing optical time division multiplexing (OTDM) technologies, the continued growth in capacity of fiber optic networks can be assured. Recent advances in OTDM have proven this technology's tremendous ability to perform high bandwidth switching among a large number of ports while offering aggregate capacities that exceed current electronic switched routers. Research groups throughout the world have begun exploring OTDM all-optical switching techniques.

## 2 All-optical devices

All-optical switches and demultiplexers are fundamental building blocks for enabling future OTDM systems [1]. Semiconductor optical nonlinearities with long recovery times ($\geq$ 100 ps) have been used to demonstrate efficient interferometric all-optical devices that promise to deliver switching and demultiplexing on terabit/s data streams. These nonlinearities are typically based upon a resonant excitation in actively-biased optical amplifiers or passive semiconductor nonlinear waveguides. Extensive experimental [2-7] and theoretical analysis [7-11] has been performed on various interferometric configurations of these devices. Due to their compact design, many of these switch architectures have been integrated, indicating their feasibility for future communication systems [12-17]. Optical nonlinearities in semiconductors are a very promising area for developing ultrafast and efficient optical switches [1]. Optical switches using actively-biased semiconductor optical amplifiers (SOAs) as the nonlinear switching element, have been used to demonstrate switching in systems using low control pulse energy (250 fJ) [18]. Although passive devices have demonstrated the shortest switching windows to date ($\sim$200 fs) [3], the passive bandfilling effect typically requires more optical control energy than actively- biased SOAs. Gain saturation induced bandfilling in active SOAs is enhanced by stimulated emission and therefore requires lower control pulse energy to generate sufficient nonlinearity for switching [16]. Also other sub-picosecond nonlinearities in semiconductors can be exploited to achieve ultrafast switching [1] and all-optical modulation [19].

### 2.1 Interferometric devices for all-optical processing

Interferometric devices for optical processing have been of great interest to the research community for some time [20] and gained momentum in the research community with the development of nonlinear optical loop mirrors (NOLMs) [21-23]. These devices, which simply consist of a 2x2 coupler and a long loop of fiber formed by joining the two fibers of one of the coupler's ends together, rely upon weak nonlinear interactions between a control and a signal pulse as they both co-propagate around the loop. If the nonlinear interaction is sufficiently large, a phase shift in the signal pulse propagating with the control pulse can be induced with respect to the counter-propagating signal pulse which does not travel with the control pulse. The change in phase alters the interference condition at the base of the loop when the signals recombine at the coupler and

switches the signal to the output port. Signals entering the loop in the absence of the control pulse, do not experience an appreciable phase change and are reflected back toward the source.

The switching windows for NOLMs can be made very short as they typically only depend upon the characteristics of the control pulse and the response of the nonlinearity. Indeed, switching experiments with temporal widths of 620 fs have been achieved [24]. However, NOLMs depend upon a weak nonlinear interaction in the fiber which usually requires high control pulse energies ($>$1 pJ) and long fiber loop lengths ($>$100 m) to generate a significant phase shift. Although there are many techniques to reduce both the control pulse energy requirements and loop lengths [23, 25], practical, compact devices for commercial optical communication systems have yet to be realized.

Finding a technique to reduce the control pulse energy and fiber lengths required in NOLMs relied upon using a nonlinear material other than fiber. Many groundbreaking experiments with semiconductor optical amplifiers (SOAs) inserted into the loop demonstrated that low energy optical pulses could change the gain of the amplifiers sufficiently to produce significant phase shifts in subsequent pulses passing through the amplifier [26]. As these integrated semiconductor amplifiers were very short ($<$1 mm) they became a practical alternative to generating an optically induced nonlinearity. Additionally, the temporal onset of the phase shift was nearly as fast as the rising edge of the control pulse [27]. Unlike non-resonant fiber nonlinearity, however, this resonant, interband nonlinearity in the semiconductor material has a long relaxation time (100 to 500 ps). Efforts were soon underway to form a new class of switching devices based upon the efficient resonant nonlinearity in SOAs to induce a differential phase change between the two signal pulses counter- propagating in the fiber loop. The first device developed was known as a semiconductor laser amplifier in a loop mirror (SLALOM) and was used to investigate "contrast enhancement and optical correlation" [28]. Although the rising edge of the temporal switching window was a few picoseconds, the window's falling edge depended upon the gain recovery time of the SOA which was approximately 400 ps [28].

The last innovation to produce picosecond switching windows with SOAs was an architectural realization. It was discovered that the temporal duration of the window could be controlled by changing the asymmetric placement of the SOA. Due to the dynamics of this configuration, the switching window actually closes *earlier* than the recovery time of the SOA as the SOA is moved closer to the midpoint. Fig. 1 shows a schematic diagram of this device known as a Terahertz Optical Asymmetric Demultiplexer (TOAD) [2]. In the absence of a control pulse, data pulses enter the fiber loop, pass through the SOA at different times as they counter-propagate around the loop, and recombine interferometrically at the coupler. Since both pulses see the same medium as they propagate around the loop, the data is reflected back toward the source. In the presence of the control pulse, switching can occur. When a control pulse is injected into the loop, it saturates the SOA and changes its index of refraction. As a result, a differential phase shift can be achieved between the two counter- propagating data pulses to switch the data pulses to the output port. Only the pulses that co-propagate with and travel just behind the control pulse by up to twice the optical path length of the SOA offset are switched to the output port. All subsequent pulses will either see an unsaturated amplifier or a slowly recovering amplifier and will be reflected back toward the source. A polarization or wavelength filter is used at the output to reject the control and pass the switched data signal. The temporal duration of the switching window is determined by the offset of the SOA, $\Delta x$, from the center position of the loop. As this offset is reduced, the switching window size decreases. The size of the nominal switching

window duration, $\tau_{win}$, is related to the offset position by $\tau_{win} = 2\Delta x/c_{fiber}$ (where $c_{fiber}$ is the speed of light in fiber).

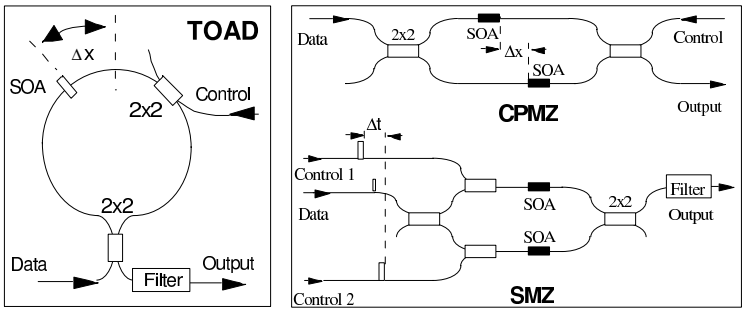


Fig. 1. Schematic diagram of ultrafast all-optical demultiplexers: a) The TOAD; b) CPMZ and SMZ.

By precisely controlling the offset position of the SOA, very short switching windows can be achieved. Demultiplexing of a single channel from a 250-Gb/s data stream has been demonstrated [29]. The practical control and data pulse energy requirements make it well-suited for typical communication signal powers. As the size of the device only depends upon the SOA length and offset from the center position in the loop, compact TOADs based upon discrete components have been constructed with loop lengths of less than 0.5 meter. The TOAD is robust to temperature variations and can be reliably operated without stabilization as data signals propagating in both directions around the loop experience the same effective medium. This device and its other variations may prove to be a practical approach to all-optical switching as they can be integrated using a variety of techniques that are discussed in this Section 2.2. The first experiments to evaluate the performance of the TOAD consisted of aggregating several pulses in time to form an ultrafast OTDM frame. Typically one pulse in the middle of the frame was modulated with a pseudorandom data pattern while the neighboring pulses were all set to 1. The demultiplexer was used to selected the modulated data signal from the ultrafast time frame. The first experiment demonstrated the TOAD's ability to switch pulses from a 50 Gb/s time frame to a baseband rate of 1.25 Gb/s [2]. This was subsequently followed by a 250 Gb/s demultiplexing experiment [29] and error-free demultiplexing from a continuous 160- Gb/s data stream [33]. Notable in all of these demonstrations was the low control pulse energy ($< 1$ pJ) needed to perform the demultiplexing function.

Although the TOAD is based upon a Sagnac interferometer, other interferometric configurations are possible using a similar operating principle. These architectures improve the integratability and performance of the device although they may require active stabilization if constructed from discrete components. Two variations of the switch in a Mach-Zehnder interferometer configuration are shown in Fig. 1b. In the absence of the control signals, the Mach-Zehnder is balanced so that data signals are rejected at the output port. When control pulses are injected into the interferometer, a differential phase shift is briefly introduced between the two arms of the interferometer causing a data pulse to be switched to the output port. Similar to the TOAD,

subsequent data pulses that pass through the switch see the slow recovery of both SOAs and are rejected. The differences between the two Mach-Zehnder geometries shown is with respect to the propagation direction of control and data signals. In the Colliding Pulse Mach-Zehnder (CPMZ) shown in Fig. 1b, the data and control signals counter-propagate through the interferometer. As a result, a filter is not needed at the output to reject the control, and the control can be coupled into the interferometer without introducing additional coupling losses. The nominal switching window for the CPMZ is determined by the distance between the midpoints of the SOAs such that $\tau_{win} = 2\Delta x/c_{fiber}$. The other architecture known as the Symmetric Mach-Zehnder (SMZ) shown in Fig. 1b requires a filter at the output port to reject the control from the switched data signal since data and control signals co-propagate. Assuming the SOAs are positioned in the same relative location within the interferometer, the nominal switching window for the SMZ is determined by the temporal control pulse separation, $\Delta t$, of Control 1 and Control 2 prior to entering the interferometer such that $\tau_{win} = \Delta t$. Although the nominal switching window size provides an estimate of the switching window temporal duration, it does not account for the finite length of the SOAs. While the SOA length has little effect on the SMZ geometry, the minimum achievable switching windows for both the TOAD and CPMZ are constrained by the length of the SOAs [7, 8]. Many theoretical models have been developed to understand the ultrafast temporal response of SOAs [27, 30-32] and the characteristics of these optical switches [7-11].

With the successful development of all-optical demultiplexing, many new techniques have been used to enhance the performance of these devices. As the optical switching function is based upon gain saturation in an SOA, the repetition rate of the demultiplexing operation is somewhat limited by the recovery time of the amplifier. Novel optical biasing techniques using CW light have significantly reduced the recovery time [34]. It has been estimated that these techniques may enable the optical switch to function at repetition rates approaching 100 GHz [35]. Other demonstrations have shown that the TOAD can be successfully used to demultiplex many wavelengths simultaneously from an aggregated OTDM/WDM data stream [36].

*Gain-Transparent SOA-Switch* Dual wavelength operation of the TOAD/SLALOM configuration known as the Gain- Transparent SOA-Switch (*GT SOA-Switch*) has been proposed and demonstrated [37]. This device (Fig. 2) uses a data signal at a longer wavelength (1.55 $\mu$m) than the control signal (1.3 $\mu$m) so that it is far from the band edge of the optical amplifier. The technique enhances the signal-to-noise ratio of the device and can improve the switching contrast at the output. The GT SOA-switch has been successfully applied as an add/drop multiplexer [37] and to simultaneous demultiplexing of several wavelength channels from an OTDM/WDM data stream [38]. On other hand dual wavelength operation of such a switch could be to difficult to implement in the real optical network.

*Ultrafast Nonlinear Interferometer (UNI)*, developed at MIT Lincoln Labs, is another ultrafast all-optical OTDM switch using an SOA as the nonlinear element in a single-arm interferometer [4] (Fig. 3). By using a long length of Birefringent (PM) Fiber to separate orthogonally polarized components of data pulses in time, a control pulse can be introduced precisely between the components of a data pulse. When these components pass through the SOA, only the data pulse whose components are separated by the control pulse will experience a differential phase change. As a result, when the pulses are realigned by another long length of PM fiber, the components will interfere with each other. Only the pulse which experiences the differential phase change induced by the control pulse will be passed to the Output through the Polarization Filter (PM Filter). Although the TOAD/SLALOM and the UNI share several characteristics, the

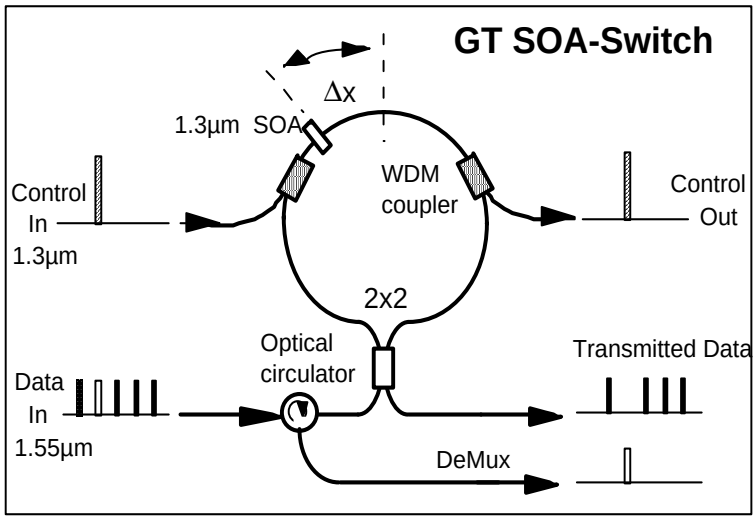


Fig. 2. GT SOA-Switch in Sagnac-interferometer TOAD/SLALOM configuration.

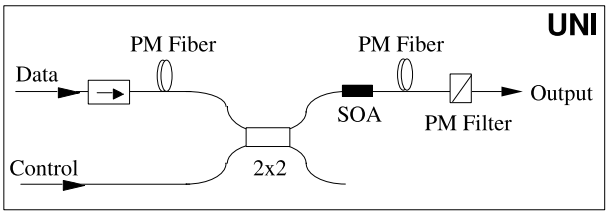


Fig. 3. Schematic diagram of Ultrafast Nonlinear Interferometer (UNI).

integratability and practicality of the UNI are limited by the long lengths of PM fiber needed to induce the polarization walk-off.

The switching window of the UNI is determined primarily by the birefringence of the PM fiber used to separate orthogonally polarized components of the data pulses in time. Enough walk-off is required to insert a control pulse between these two pulses. At a minimum, the walk-off should be longer than the control pulse width. Like any other SOA based switch, the UNI is limited by intraband carrier dynamics and carrier heating. Switching windows of about 1 ps can be expected. The switching repetition rate can be limited by the carrier recombination time in the SOA. However, 100 GHz repetition rates for bitwise logic functions have been reported [39]. As with any SOA-based switch, the UNI also has a noise background added to the switched signal due to spontaneous emission from the SOA. Noise figures in the range of 6 dB are typical for SOAs. Filtering and other techniques can be used to reduce the accumulation of noise in the signal for cascaded devices. Since the UNI requires at least 15 m of PM fiber to produce

the switching window [4], it is not likely that it will be easy to integrate. Since the UNI is dependent upon birefringence to achieve switching, the system must use extensive polarization control throughout the network to maintain reliability.

*Nonlinear Waveguide (NLWG) Switch.* Record breaking optical demultiplexing has recently been reported by a group at NEC Research working on a device known as a nonlinear waveguide (NLWG) switch. The group achieved 1.5 Tb/s demultiplexing with a 200 fs switching window at a repetition rate of 10 GHz [3]. The devices uses a Mach-Zehnder interferometer configuration and passive semiconductor waveguides spatially offset within the arms to produce switching. This approach is very similar to the SMZ-TOAD configuration except that the semiconductor nonlinear waveguides are not actively biased. The NLWG switch uses data and control pulses sufficiently separated in wavelength to produce a bandfilling effect in the semiconductor waveguide. First, an interferometer is built using NLWGs in the arms (this may include a Sagnac, Mach-Zehnder, or even single-arm interferometer like the UNI). When a control pulse is introduced into the device at an appropriate wavelength, it is absorbed by the NLWG. The absorption creates an instantaneous refractive index change in the material through the bandfilling effect. Subsequently, data pulses which traverse the NLWG immediately after the control pulse can experience a differential phase change needed to produce switching and demultiplexing. The data and control pulses, which have different wavelengths, are separated at the output of the device using a bandpass filter. The switching window achieved in the most recent demonstration of the NLWG switch is the shortest to date ($\sim$200 fs). The small temporal window is a result of the nearly instantaneous index change of the semiconductor material from the control pulse. Unlike active SOA-based demultiplexers, the NLWG is a passive structure which does not exhibit intraband carrier dynamics or carrier heating. The nonlinear response can be almost as fast as the rising edge of the control pulse. The control pulse energy requirement of the NLWG device is one of its major limitations. Since the NLWG is passive, a significant amount of photons must be absorbed in the material to achieve an adequate phase shift for switching. For the InGaAsP waveguides at 1.55 $\mu$m, a control pulse of nearly 5 pJ is required (after accounting fiber-to-chip coupling losses). To date, coupling efficiencies of only 10% have been achieved. As a result, a system built with NLWG demultiplexers would require control pulse energies of almost 50 pJ. Since the NLWG is passive, it is not likely that the control pulse energy can be reduced much beyond a few tens of picojoules. This greatly limits the device application to practical systems. Noise figure of a passive switch is typically not a problem and estimated to be less than 2 dB for these devices. Switching repetition rates of 40 GHz have been experimentally demonstrated by the NEC group [40].

### 2.2 Integration of All-Optical devices

We briefly review the progress that has been made in this area. While all of discussed devices presented can be constructed from discrete components, practical, high performance all-optical switches for commercial systems will most likely take advantage of photonic integration technology.

*Integrated all-optical switches.* The Sagnac, Mach-Zehnder, and Michelson interferometer all-optical switch geometries have been integrated by various groups. In order to fabricate these devices, both monolithic and hybrid technologies have been used. The first monolithically integrated nonlinear Sagnac interferometer capable of demultiplexing from 20 Gb/s to 10 Gb/s or 5

Gb/s was demonstrated by the Heinrich Hertz Institute (HHI) in 1996 [12]. Both the colliding pulse Mach- Zehnder (CPMZ) and symmetric Mach-Zehnder (SMZ) geometries have been integrated and subsequently demonstrated as high-speed demultiplexers by many groups [13-16]. Although the Mach-Zehnder configuration requires additional SOAs and couplers as compared to the Sagnac device, the Mach-Zehnder structures are more practical to fabricate since they do not require a large loop radius which may lead to bending losses in the waveguides. Furthermore, the SMZ has the inherent advantage that it exhibits the shortest switching window in the co-propagating configuration. Finally, an SOA-based optical switch using an integrated Michelson interferometer was used to demonstrate demultiplexing from 20 to 5 Gb/s [17]. The Michelson configuration may be a practical approach to integrated switching as anti-reflection coating is only applied to one side of the device and only two fiber-to-chip couplings are necessary for its operation as a demultiplexer [17].

The highest performance for demultiplexing has been demonstrated using the Mach-Zehnder structures. Both the CPMZ fabricated by HHI and the SMZ fabricated by Alcatel have been used to optically demultiplex from 40 to 10 Gb/s [13, 14]. The Alcatel monolithic SMZ is an all-active device as all waveguides contain an active SOA element fabricated on the same substrate. This device improves the optical power requirements by providing additional gain to account for fiber-to-chip coupling losses. A high performance monolithically integrated SMZ was also demonstrated by a collaboration among the Swiss Federal Institute of Technology, University of Denmark, and France Telecom. This group achieved reliable demultiplexing from 80 to 10 Gb/s [15]. The highest performance for an integrated SMZ to date has been achieved using a hybrid technique employed by NEC [16]. Fiber guides and passive silica waveguides are first fabricated onto a silicon planar lightwave circuit (PLC). The active SOA array chip is then flip chip mounted onto the PLC. Recently, NEC used this chip to demonstrate demultiplexing from 168 Gb/s to 10 Gb/s [16]. As integration technology in this area continues to mature, deployment of high performance optical switches in commercial systems becomes possible.

*Integrated all optical wavelength converter.* Wavelength conversion is one of the key functions which must be performed in existing DWDM optical networks. In current optical networks in order to perform conversion from wavelength $\lambda_1$ to wavelength $\lambda_2$, an optical signal at $\lambda_1$ must be first detected by a photoreceiver, then converted into an RF signal. This RF signal is now used to modulate a cw DFB laser to generate the required data at the new wavelength $\lambda_2$. This process is relatively slow and creates electronic bottlenecks in existing systems. This can be avoided if wavelength conversion is done all-optically for example using newly developed Integrated All-Optical Wavelength Converter 1901 ICM from Alcatel. Fig. 3 is a schematic diagram of such a device. This converter exploits cross-phase modulation in an integrated Mach- Zehnder (MZ) interferometer based on an all-active MZ-SOA structure. An input modulated signal at a wavelength $\lambda_1$ modulates the carrier density in the SOA inside of the interferometer, producing a modulation of its refractive index. This in turn leads to phase modulation of an injected CW beam at the desired output wavelength $\lambda_2$, which is converted to amplitude modulation via the MZ interferometer. The signal data pattern is therefore transferred to the new wavelength $\lambda_2$.

The nonlinear transfer function of the device allows both enhancement of the signal extinction ratio and compression of the optical noise amplitude.

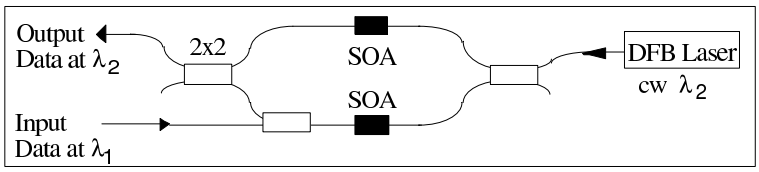


Fig. 4. All-Optical Interferometric Wavelength Converter - schematic diagram.

## 3 Opto-mechanical switching devices

While the previous analysis in Chapter 2 only considered interferometric based all-optical switches, other mechanisms for optical switching are also being pursued vigorously. The most common optical switching fabric that is currently being integrated into commercial packet switching systems is based upon micro-electro-mechanical systems or MEMS. Simple embodiments of the MEMS technology include movable micro-mirrors that route beams of light according to their destination. Early this year Agilent Technologies gained a lot of attention by announcing its capability to use a bubble technology for optical switching and routing. These two promising technologies are discussed in this section.

### 3.1 Movable Mirror Architectures

One of the leader in MEMS technology today is Lucent Technologies. Lucent is poised to offer their first all-optical routing system this year called the WaveStar LambdaRouter. The LambdaRouter uses a 256x256 array of movable mirrors to direct light from one fiber to another. Advantages of the MEMS architecture include scalability, low power consumption, low loss, compact size, and protocol transparency. Lucent's current system can support single channel data rates as high as 40 Gb/s. MEMS offers a simple solution to the optical switching problem and avoids the electronic conversion required in standard routers but the applications area is somewhat limited. Since MEMS are inherently mechanical, they are limited in speed. The Lucent LambdaRouter can move its mirrors only on a time scale of 10 ms. While this is appropriate for optical circuit switching and optical layer restoration protection switching, it is not nearly fast enough to support switching on a packet-by-packet basis required by IP routing. Furthermore electronic hardware must still be used to obtain the routing information to control the switch. Due to the mechanical nature of MEMS, long-term reliability and packaging are still critical issues in these systems that will be proved over time. Additional advances in MEMS will most likely be able to upgrade the speed of these switches. The MEMS based switches will most likely interconnect service providers and large cities where continuous traffic streams are established for longer periods of time between fixed locations.

### 3.2 Bubble Technology

Agilent Technologies has been a pioneer of ink-jet technology for low-cost color printers. This same technology has now been applied to an all-optical switch fabric and commercial systems

are expected by the end of year 2000. The current prototype demonstration is a 32x32 all-optical switching matrix. These new photonic switches are based on technology that uses a combination of reliable inkjet and planar lightwave circuit technologies. They accomplish the task of re-directing light without the help of mirrors or any other moving parts. This switch is composed of a vertical and horizontal array of permanently aligned waveguides. Light is transmitted across a horizontal path from the input to output port until a switch command is issued. When commanded, a bubble is created at the intersection of appropriate waveguides and the light is reflected down a vertical path to the switched port. This bubble is formed using the same reliable technology now used in inkjet printers. Like MEMS, bubble technology has low loss, format and protocol transparency, and compact size. The bubble technology may prove to be more reliable than MEMS based switches since there is less moving parts involved in the switching operation. Little information is available about the capabilities of this new, proprietary technology. It is estimated based upon the ink-jet printing technology, that switching latency will fall in the millisecond range. The Agilent switch might find applications in optical circuit switching and optical layer restoration protection switching.

## 4 Conclusions

Although electronics has made great strides toward satisfying the switching bandwidth of future communication networks, it does not appear that electronic switches will reach the targeted terabit/second regime even with the highest degree of parallelism. However, based on presented results these newly developing technologies might provide a revolutionary breakthrough in scalability, bandwidth, reliability, and speed. In conclusion, Table I summarizes the key device parameters of the technologies presented in this paper.

Table I. Comparison of four types of optical switches.

| Device | Switching Time | Repetition Rate | Control Pulse Energy (pJ) | Noise Figure (dB) | Integrat. |
|---|---|---|---|---|---|
| TOAD/SLALOM | $<$ 1 ps | 100+ GHz | 0.25 | 6 | YES |
| UNI | $<$ 1 ps | 100+ GHz | 0.25 | 6 | NO |
| NLWG | 0.2 ps | 40+ GHz | 50 | low | YES |
| NOLM | 0.8 ps | 100+ GHz | 50+ | low | NO |
| MEMS | 10 ms | $<$ 1 kHz | N/A | N/A | YES |
| Bubble | 10 ms | $<$ 1 kHz | N/A | N/A | YES |

### References

[1] O. Wada: *Opt. Quant. Electron.* **32** (2000) 453

[2] J. P. Sokoloff, P. R. Prucnal, I. Glesk, M. Kane: *A Terahertz Optical Asymmetric Demultiplexer (TOAD), OSA Proceedings on Photonics in Switching*, (Eds. J. W. Goodman, R. C. Alferness) Optical Society of America, Washington, D.C. 1993 **16**, PD-4; J. P. Sokoloff, P. R. Prucnal, I. Glesk, M. Kane: *IEEE Photon. Technol. Lett.* **5** (1993) 787

[3] S. Nakamura, Y. Ueno, K. Tajima: *IEEE Photon. Technol. Lett.* **10** (1998) 1575

[4] N. S. Patel, K. L. Hall, K. A. Rauschenbach: *Optics Lett.* **21** (1996) 1466

[5] A. D. Ellis, D. M. Patrick, D. Flannery, R. J. Manning, D. A. O. Davies, D. M. Spirit: *J. Lightwave Technol.* **13** (1995) 761

[6] M. Eiselt, W. Pieper, H. G. Weber: *Electron. Lett.* **29** (1993) 1167

[7] P. Toliver, R. J. Runser, I. Glesk, P. R. Prucnal: *Optics Comm.* **175** (2000) 365

[8] K. I. Kang, T. G. Chang, I. Glesk, P. R. Prucnal: *Appl. Opt.* **35** (1996) 417

[9] R. J. Manning, A. D. Ellis, A. J. Poustie, K. J. Blow: *J. Opt. Soc. Am. B* **14** (1997) 3204

[10] N. S. Patel, K. L. Hall, K. A. Rauschenbach: *Appl. Optics* **37** (1998) 2831

[11] S. Nakamura, K. Tajima: *Jpn. J. Appl. Phys.* **35** (1996) L1426

[12] E. Jahn, N. Agrawal, W. Pieper, H.-J. Ehrke, D. Franke, W. Furst, C. M. Weinert: *Electron. Lett.* **32** (1996) 782

[13] E. Jahn, N. Agrawal, M. Arbert, H.-J. Ehrke, D. Franke: *Electron. Lett.* **31** (1995) 1857

[14] D. Wolfson, A. Kloch, T. Fjelde, C. Janz, B. Dagens, M. Renaud: *IEEE Photon. Technol. Lett.* **12** (2000) 332

[15] R. Hess, M. Caraccia-Gross, W. Vogt, E. Gamper, P. A. Besse, M. Duelk, E. Gini, H. Melchior, B. Mikkelsen, M. Vaa, K. S. Jepsen, K. E. Stubkjaer, S. Bouchoule: *IEEE Photon. Technol. Lett.* **10** (1998) 165

[16] K. Tajima, S. Nakamura, Y. Ueno, J. Sasaki, T. Sugimoto, T. Kato, T. Shimoda, H. Hatakeyama, T. Tamanuki, T. Sasaki: *IEICE Trans. on Electron. E* **83C** (2000) 959

[17] B. Mikkelsen, M. Vaa, N. Storkfelt, T. Durhuus, C. Joergensen, R. J. S. Pedersen, S. L. Danielsen, K. E. Stubjaer, M. Gustavsson, W. van Berlo:*Monolithic integrated Michelson interferometer with SOAs for high-speed all-optical signal processing, Proc. OFC'95* San Diego, CA 1995, pp. 13-14, paper TuD4

[18] K.-L. Deng, R. J. Runser, P. Toliver, C. Coldwell, D. Zhou, I. Glesk, P. R. Prucnal: *Electron. Lett.* **34** (1998) 2418

[19] Neogi, O. Wada, Y. Takahashi, H. Kawaguchi: *Opt. Lett.* **23** (1998) 1212

[20] K. Otsuka: *Opt. Lett.* **8** (1983) 471

[21] N. J. Doran, D. Wood: *Opt. Lett.* **13** (1988) 56

[22] N. J. Doran, D. S. Forrester, B. K. Nayar: *Electron. Lett.* **25** (1989) 267

[23] M. Jinno, T. Matsumoto: *Opt. Lett.* **16** (1991) 220

[24] E. Yamada, K. Suzuki, M. Nakazawa: *Electron. Lett.* **30** (1994) 1966

[25] M. Asobe, T. Ohara, I. Yokohama, T. Kaino: *Electron. Lett.* **32** (1996) 1396

[26] A. W. O'Neill, R. P. Webb: *Electron. Lett.* **26** (1990) 2008

[27] J. Mark, J. Mork: *Appl. Phys. Lett.* **61** (1992) 2281

[28] M. Eiselt: *Electron. Lett.* **28** (1992) 1505

[29] I. Glesk, J. P. Sokoloff, P. R. Prucnal: *Electron. Lett.* **30** (1994) 339

[30] K. L. Hall, G. Lenz, A. M. Darwish, E. P. Ippen: *Opt. Comm.* **111** (1994) 589

[31] J. M. Tang, K. A. Shore: *IEEE J. Quantum Electron.* **34** (1998) 1263

[32] M. Y. Hong, Y. H. Chang, A. Dienes, J. P. Heritage, P. J. Delfyett: *IEEE J. Quantum Electron.* **30** (1994) 1122

[33] K. Suzuki, K. Iwatsuki, S. Nishi, M. Saruwatari: *Electron. Lett.* **30** (1994) 1501

[34] R. J. Manning, D. A. O. Davies: *Opt. Lett.* **19** (1994) 889

[35] R. J. Manning, D. A. O. Davies, D. Cotter, J. K. Lucek: *Electron. Lett.* **30** (1994) 787

[36] B. K. Mathason, H. Shi, I. Nitta, J. Abeles, J. C. Connolly, P. J. Delfyett: *IEEE Photon. Technol. Lett.* **11** (1999) 331

[37] S. Diez, R. Ludwig, H. G. Weber: *IEEE Photon. Technol. Lett.* **11** (1999) 60

[38] S. Diez, R. Ludwig, H. G. Weber: *Electron. Lett.* **34** (1998) 803

[39] K. L. Hall, K. A. Rauschenbach: *Opt. Lett.* **23** (1998) 1271

[40] K. Tajima, S. Nakamura, Y. Ueno: *Mat. Sci. Eng. B - Solid B* **48** (1997) 88